14

Tunable Fibre Lasers Based on Optical Amplifiers and an Opto-VLSI Processor

Feng Xiao[1], Kamal Alameh[1,2] and Yong Tak Lee[2,3]
[1]*Electron Science Research Institute, Edith Cowan University,*
[2]*Department of Nanobio Materials and Electronics,*
Gwangju Institute of Science and Technology,
[3]*Department of Information and Communications,*
Gwangju Institute of Science and Technology,
[1]*Australia*
[2,3]*Korea*

1. Introduction

Tunable lasers are currently used in a wide range of applications such as wavelength-division-multiplexing networks, optical sensors, spectroscopy, wavelength protection, fiber-optic gyroscope, and testing of optical components and instruments. In particular, tunable fiber lasers, which employ optical fiber cavity and wave-guided gain medium, have recently attracted great interest owing to several intrinsic advantages over traditional lasers, namely: (i) easy manufacture without the need of clean rooms and expensive device packaging; (ii) mechanical flexibility and the ability to withstand bending, thus opening the way for numerous applications in biotechnologies and medical instrumentation; (iii) broadband gain spectrum and high energy efficiency, which are very important features for tunable high-power lasers; (iv) high laser beam quality, ensuring their wide potential applications in material processing, printing, marking, cutting and drilling; (v) robustness, because all optical signals are guided within optical fibres, thus eliminating the need for optical alignment; and (vi) narrow line width which is essential for many applications and hard to achieve for their current counterparts. Benefiting greatly from recent developments in fibre communications, fibre lasers are offering a low-cost alternative to the traditional semiconductor or gain dielectric counterparts.

The key features required for tunable fiber lasers include a large number of channels, high--output power, stable operation in power and wavelength, and tuning operation over a wide wavelength range with application-specific wavelength spacing. However, the current fibre lasers, especially multiwavelength fiber lasers, suffer from limited tunability and flexibility, poor stability, and narrow operation ranges.

Two main aspects related to the development of tunable single/multiwavelength fibre lasers are currently under intensive investigation; namely, the wavelength selection (or tuning) mechanism, and the used gain media. While these investigations have resulted in significant progress towards the development of commercially viable products each of the current approaches have particular limitations.

In this Chapter, we discuss the use of Opto-VLSI processors for the development of tunable fiber lasers. Section 2 briefly reviews the recent progress in tuning mechanism for single and multiple wavelength tuning. Section 3 discusses different approaches for implementing the gain media of fiber lasers. In Section 4 a brief background on Opto-VLSI processors is provided. Single-wavelength, multi-wavelength and multiport tunable fiber lasers employing Opto-VLSI processors are presented in Sections 5, 6 and 7, respectively. We conclude this chapter in Section 8.

2. Tuning mechanism

2.1 Single-wavelength tuning

The tunable single-wavelength fiber laser is relatively mature compared to its multiwavelength countparts. However, due to its long cavity, which is able to give narrow linewidths, a fiber laser oscillates on multiple longitudinal modes (A. Bellemare *et al.*, 2001). Mode discrimination by the gain medium is not strong enough to restrict the oscillation to a single longitudinal mode, despite the fact that homogeneous broadening is known to dominate in gain media, such as erbium-doped fibers, at room temperature. Therefore, one or more spectrally discriminating elements or very short cavities should be employed to limit the number of modes over which the laser may effectively oscillate. Nevertheless, this does not ensure the oscillation of one longitudinal mode (Park *et al.*, 1991).

To suppress multimode lasing as well as mode hopping, technologies including the use of cascaded bandpass filters (one narrow and one broad) (Park *et al.*, 1991; Chow *et al.*, 2002) and a passive multiple-ring cavity (C. C. Lee *et al.*, 1998) have commonly been used. More importantly, an unpumped Er^{3+}-doped fiber has been incorporated in a long Fabry–Perot laser cavity as a saturable absorber to establish linewidth narrowing and single-mode operation (Cheng *et al.*, 1995). In addition, the beat-noise of fiber ring lasers, which is primarily in the low-frequency region of about 10 MHz due to the long ring cavity length, has successfully been suppressed by inserting a Fabry–Pérot laser diode (FP-LD). (H. L. Liu *et al.*, 2006).

Several single-wavelength tuning mechanisms have been intensively investigated. Some early works on single-wavelength tuning have been demonstrated using intracavity elements such as gratings or birefringent plates, whose orientation can be changed mechanically. In order to switch the wavelength electrically, the use of bulk electro-optic intracavity tuners, such as liquid crystal cells, has been reported (MOLLIER *et al.*, 1995), where the tuning range of the device was 17 nm and the tuning rate was 8 nm/V.

A tunable single-longitudinal-mode compound-ring Er3+-doped fiber laser has been demonstrated (J. L. Zhang *et al.*, 1996; C. C. Lee *et al.*, 1998), where the laser is fundamentally structured on an all-fiber compound-ring resonator in which a dual-coupler fiber ring is inserted into the main cavity. When combined in tandem with a mode-restricting intracavity tunable bandpass filter, the compound-ring resonator ensures single-longitudinal-mode laser oscillation. The laser can be tuned over much of its 1525 to 1570 nm wavelength tuning range with the short-term linewidth of less than 5 kHz.

Acousto-optic tunable filters (AOTFs) have recently been used as a wavelength selector because of their broad tuning ranges, narrow bandwidths, simple tuning mechanisms, and low drive power requirements (Chang *et al.*, 2001; Kang *et al.*, 2006). A single-frequency tunable fiber ring laser incorporating an all-fiber acousto-optic tunable bandpass filters (AOTBFs) has been characterized in detail and the impact of the AOTBF characteristics on the laser performance has also been examined (Kang *et al.*, 2006). The AOTBF consists of an

all-single-mode-fiber acousto-optic tunable filter and a core-mode blocker in the center of the acousto-optic interaction region. Stable single-longitudinal-mode operation has been achieved over the wavelength range of 48 nm with a side mode suppression ratio higher than 50 dB.

The use of tunable fiber Bragg gratings (FBGs) is a simple approach to realize single-wavelength tuning (Song *et al.*, 2001). Recently, a tunable fiber laser based on a tunable phase-shifted linearly chirped FBG (PS-LCFBG) in transmission with ultra-narrow bandwidth of 1.52 kHz has been demonstrated (Li *et al.*, 2008). By thermally tuning the transmissive PS-LCFBG, a tuning range of 15.5 nm was obtained. A tunable L-band fiber laser based on a mechanically induced LPFG into the EDF ring has been demonstrated (Sakata *et al.*, 2009). Wavelength tuning was achieved by adjusting the grating period to shift the rejection band against the ASE spectrum of the ring cavity. Although thermal effects on the laser were controlled, this technique suffers from the environmental disturbances.

Tunable fiber Fabry–Perot filters have widely been utilized as tuning elements in tunable lasers (X. Y. Dong *et al.*, 2003; Zheng *et al.*, 2006; Chien *et al.*, 2005b; Chien *et al.*, 2005a; Fu *et al.*, 2009). A fiber laser utilizing a tunable fiber Fabry–Perot filter as the tuning element has been demonstrated, which had a moderate milli-Watt level power output over almost the whole tuning range from 1530 to 1595 nm with power fluctuations less than 0.15 dB (Fu *et al.*, 2009). High repetition scanning rate of laser operation over the whole tuning range was achieved at rates of up to 200Hz. The limited tuning range of this tunable filter could be extended by incorporating another tunable passband filter. A tunable narrow-bandpass fiber Fabry-Perot (FFP) filter with a bandwidth of 0.2 nm and free spectral range (FSR) of 28 nm combined with six bandpass filters (BPFs) of 20 nm bandwidth has been used as a wide tuning component (X. Y. Dong *et al.*, 2003). Only one of the BPFs was turned on at a time. Since the bandwidth of each BPF was less than the FFP's 28-nm FSR, continuous wavelength tuning was obtained within a 20 nm range by changing the voltage applied to the piezoelectric transducer of the FFP, thus attaining a total tuning range of 120 nm.

Based on the use of a narrow-band tunable microelectromechanical system (MEMS) filter, a wide-band short-cavity length tunable fiber ring laser that can be tuned at high speed from 1520 to 1626 nm has been reported (H. L. Liu *et al.*, 2005a). The optical bandwidth of the MEMS was about 20 pm (2.5 GHz) tuned over 120 nm, from 1630 to 1510 nm by varying the input voltage from 10 to 32 V, respectively. The MEMS filter also exhibited very high scanning speed (greater than 100 000 nm/s). The insertion loss of the MEMS filter at the peak of the passband was less than 1.5 dB, and the out-of-band reflection from both ends of the MEMS filter was as high as 95%.

Lyot filters, which are a type of optical filter that uses birefringence to produce a narrow passband of transmitted wavelengths, have also been used to widely tunable fiber lasers (Zhou *et al.*, 1998; Xu *et al.*, 2002). The semiconductor fiber ring laser utilized the birefringence of optical fibers, especially PM fiber, together with the polarization controller, rotating linear polarizer and SOA, to form polarization-dependent loss and gain mechanisms. For this filter, different wavelengths arrive at the linear polarizer and SOA with different polarization states due to birefringent chromatic dispersion in the cavity, hence, different wavelengths have different losses due to the polarization dependent loss through the linear polarizer. A wavelength with its electrical field vector lined up with the linear polarizer experiences the least loss. The combination of a polarization controller and linear polarizer thus provided a wavelength selection mechanism to generate a tunable laser

output. In addition, as the gains of the SOA are different for transverse electrical (TE) fields and transverse magnetic (TM) fields, 3-dB gain difference between TE and TM polarizations were experienced in addition to gain differences due to the SOA spectrum itself. This also provided gain discrimination due to the fact that different wavelengths have different input polarization states at the SOA. Therefore, the combination of the intracavity polarization controller, the polarizer, and the SOA served as wavelength selection mechanisms. Thus, the lasing wavelength is the light wave that repeats its state of polarization in front of both the polarizer and the SOA after one round-trip and whose polarization state lines up with the linear polarizer and TE or TM direction within the SOA whichever has a higher gain.

2.1 Multi-wavelength tuning

Multiwavelength tuning is much more complex compared to single wavelength tuning, and recently it has attracted equal attention from all over the academic society. Several versatile techniques to realize multi-wavelength tuning have been proposed and demonstrated. A spatial mode beating filter has been reported, which can tune a multiwavelength fiber laser by simply incorporating a section of multimode optical fiber into a single-mode fiber ring cavity (Poustie *et al*., 1994). This combination of two fiber types results in wavelength-dependent filtering action inside the laser cavity arising from the spatial mode beating between the LP01 and LP11 modes in the multimode fiber. The multiwavelength fiber laser can be tuned by controlling the polarization controller in the fiber loop.

Tunable FBGs are still the commonly-used technology for multiwavelenth tuning (Han *et al*., 2007; Liaw *et al*., 2007; Alvarez-Chavez *et al*., 2007; Moon *et al*., 2005). A spacing-tunable multiwavelength Raman fiber laser with an independently-adjustable channel number, based on a superimposed chirped-fiber Bragg grating (CFBG) and a linear cavity formed by a bandwidth-tunable CFBG reflector, has been demonstrated (X. Y. Dong *et al*., 2006). Multiwavelength laser operations at room temperature with spacing of 0.3 to 0.6 nm, and channel number of 2 to 10 have been achieved.

Recently a tunable multiwavelength fiber laser based on an all-fiber FP filter which is constructed by a superimposed CFBG has been demonstrated (Han *et al*., 2007). The FP filter is capable of continuous FSR tenability, through incorporating a specially designed apparatus for induction of the sophisticated bending along the grating. The proposed technique is based on the symmetrical modification of the chirp ratio along the fiber grating attached on a flexible cantilever beam. The FSR of the all-fiber FP filter could be continuously tuned from 0.21 to 0.81 nm with neglect center wavelength shift.

A fiber loop mirror incorporating a piece of polarization maintaining fiber (PMF) has attracted much attention as an optical comb filter due to its intrinsic advantages such as easy fabrication, stability and flexibility (Z. X. Zhang *et al*., 2009). The PMF-based fiber loop mirror filters can provide various functionalities like both the peak wavelength tunability and FSR tunability, which can be controlled by adjusting the effective length and birefringence of multiple PMF segments depending on the relative phase difference between two orthogonal polarization modes within the loop (Kim *et al*., 2003; Z. Y. Liu *et al*., 2008). The comb filter can also be tuned by changing the operating temperature or by applying axial strain to the PMF (Moon *et al*., 2007). Besides these, an active device such as a phase modulator (Fok *et al*., 2005) or SOA (K. L. Lee *et al*., 2004) is also inserted in the fiber loop mirror to tailor the effective birefringence of the loop, enabling continuous shift of the transmission comb spectrum.

Unlike the use of passive single-mode PMFs into the Sagnac loop, a tunable transmission comb filter based on a pumped erbium-ytterbium co-doped polarization maintaining fiber (EYD-PMF) loop mirror has been recently demonstrated (G. Y. Sun *et al.*, 2008). The effective birefringence of the EYD-PMF depends on the power of pump lasers and the polarization state of the traversing signal. Therefore, the comb filter can be tuned by changing the pump power or adjusting a PC adjacent to the EYD-PMF in the loop.

Mach-Zehnder interferometers also offer a tuning mechanism for tunable fiber lasers (H. Dong *et al.*, 2005a). However, they usually suffer from performance instability and difficulty in free spectral range (FSR) control. A multi-wavelength fiber ring laser of tunable channel spacing has been proposed by employing an optical variable delay line (OVDL) in a Mach-Zehnder interferometer (D. R. Chen *et al.*, 2007). The channel spacing of the present multi-wavelength fiber ring laser can be continuously tuned by adjusting the computer-controlled OVDL. Multi-wavelength lasing with standard ITU channel spacing of 25 GHz, 50 GHz and 100 GHz has been demonstrated. Also, a tunable and switchable multiwavelength erbium-doped fiber ring laser based on a modified dual-pass Mach–Zehnder interferometer has been reported (Luo *et al.*, 2009). Through polarization control, the dual-function operation of the channel-spacing tunability and the wavelength interleaving can be achieved. Up to 29 stable lasing lines with 0.4 nm spacing and 14 lasing wavelengths with 0.8 nm spacing in 3 dB bandwidth were obtained.

Wavelength tunability can also be obtained through the use of a thin film tunable filter (Ummy *et al.*, 2009). A widely tunable (30 nm) fiber laser based on two Sagnac loop mirrors and a tunable thin film filter has been demonstrated, where optical power adjustability is accomplished by proper adjustment of each of the loop mirror reflectivity via a polarization controller.

3. Gain medium

3.1 Single gain medium

Many gain media are suitable for single-wavelength lasing in a fiber cavity, including erbium-doped fiber amplifiers (EDFA) (Antoine Bellemare, 2003), semiconductor optical amplifiers (SOA) (Ummy *et al.*, 2009), and hybrid gain media (Yeh&Chi, 2005). SOA-based fiber ring lasers have limited optical signal-to-noise ratio (OSNR), while EDFAs are ideal for single-wavelength tunable fiber ring lasers.

Erbium-doped fiber lasers (EDFLs) have extensively been studied as a very promising solution because EDF offers several advantages over the other gain media, such as high conversion efficiency, low threshold, homogeneous gain property thus high OSNR, narrow linewidth, coverage of the entire (C L)-band, ease of construction, and low cost (X. Y. Dong *et al.*, 2005b; A. Bellemare *et al.*, 2001; Roy *et al.*, 2005). Both theoretical and experimental investigations on how the laser performances are affected by the various parameters in the lasing cavity, such as the intracavity loss, erbium ion clustering, output coupling ratio (or reflectivity of output coupler), and active fiber length, have been carried out based on different theoretical models.

Meanwhile, some improved gain media based on EDF have also been investigated. A ring laser with 106-nm tuning range has been demonstrated based on a La-codoped Bi-EDF with about 84.6 cm long and doped with very high concentration of erbium ions (H. L. Liu *et al.*, 2005a). The erbium concentration in the Bi-EDF is 6470 wt-ppm and the La concentration is 4.4% wt. The peak absorption of the Bi-EDF at 1480 and 1530 nm are 167 and 267 dB/m,

respectively. The La ions extend the distance between Er ions and reduce the concentration quenching significantly. More recently, a Bi2O3-based erbium-doped fiber (BIEDF) ring laser with a 134 nm tunable range has been reported with only 0.2m of BIEDF as a gain media (Ohara&Sugimoto, 2008). The tunable range varies depending on both pump power and BIEDF lengths, and a high optical signal-to-noise ratio of over 70 dB for a 120 nm tunable range has been obtained.
A GeO-doped high-power and widely tunable all-fiber Raman laser using a linear cavity configuration has been demonstrated (Belanger *et al.*, 2008). The RFL was continuously tuned over 60 nm, from 1075 to 1135 nm and provided up to 5 W of Stokes output power for 6.5 W of launched pump power (LPP).

3.2 Multiple gain medium

Different gain mechanisms and media have been used to develop multiwavelength lasers, such as EDFAs (A. Bellemare *et al.*, 2000; X. M. Liu *et al.*, 2005b), SOAs (Pleros *et al.*, 2002), and schemes based on stimulated Raman scattering (SRS) gain (Kim *et al.*, 2003) and stimulated Brillouin scattering (SBS) gain (Nasir *et al.*, 2009). In addition, hybrid gain mechanisms using a combination of the above mechanisms have also been used (Han *et al.*, 2005).
The homogeneous linewidth broadening of the EDF medium limits the narrowest wavelength spacing between adjacent lasing wavelengths to a few nanometers (A. Bellemare *et al.*, 2000). To overcome this limit, various schemes such as cryogenic cooling (Yamashita&Hotate, 1996), frequency shifting (A. Bellemare *et al.*, 2000), careful gain equalization, spatial-spectral multiplexing, polarization anisotropic gain effects (Das&Lit, 2002), polarization-hole burning (J. Q. Sun *et al.*, 2000; Qian *et al.*, 2008), and intracavity four-wave mixing in nonlinear fibers (Tran *et al.*, 2008; Han *et al.*, 2006), have been used, adding more complexity (and therefore, cost) to these multiwavelength tunable lasers.
A nonlinear optical loop mirror (NOLM) based on a highly nonlinear dispersion shifted fiber has been implemented in the ring laser cavity to stabilize the multiwavelength output at room temperature (Tran *et al.*, 2008; Han *et al.*, 2006). Since the energy transfer from the higher-power waves to the lower-power waves is induced by several degenerate four-wave mixing (FWM) processes, the mode competition of the EDF is degraded. Consequently, the homogeneous line broadening of the EDF can dynamically be suppressed, leading to a stable multiwavelength output at room temperature. The FWM effects induced by the highly-nonlinear DSF introduce a dynamic gain flattening, so that the mode competition is suppressed effectively. The lasing wavelengths can be switched individually by two PCs because the nonlinear polarization phenomenon based on the NOLM induces the polarization-dependence loss and the birefringence-induced wavelength-dependent loss in the laser ring cavity, which can determine the total loss of the laser ring cavity.
Stable multiwavelength lasing has been achieved at room temperature with the hybrid gains of a Raman gain medium and an Erbium-doped fiber in a ring structure (D. R. Chen *et al.*, 2007). The multi-wavelength fiber laser employing Raman and EDF gains increases the lasing bandwidth compared with a pure EDF laser and the power conversion efficiency compared with a pure fiber Raman laser. No special fibers are needed in this proposed fiber laser structure.
SOA-based multiwavelength fiber lasers have more advantages over multiwavelength lasers with erbium-doped fiber amplifiers (H. X. Chen, 2005). This is because the SOA has a dominant property of inhomogeneous broadening and can support many wavelength lasing

oscillations simultaneously in the laser cavity, allowing narrower spacing for multiwavelength lasing operation (Qian *et al.*, 2008). A mechanism of multiwavelength generation based on nonlinear polarization rotation in an SOA has been reported (Z. X. Zhang *et al.*, 2009; Z. X. Zhang *et al.*, 2008). The arbitrarily polarized light incident to the SOA can be decomposed as the transverse electric (TE) and transverse magnetic (TM) modes. The modes propagate independently through the SOA, but they have indirect interaction via the carriers. The gain saturation of the TE mode differs from the gain saturation of the TM mode. Hence, the refractive index change of the TE mode also differs from the refractive index change of the TM mode. A phase difference between the two modes builds up as the light propagates through the SOA. A polarization controller (PC) is used to adjust the polarization of the input signal to the SOA so that the phase difference between the modes can be varied. At the following polarization-dependent isolator (PDI), both modes recombine. Another PC is used to adjust the polarization of the SOA output with respect to the orientation of the PDI. The phase difference and the orientation of the two PCs determine the intensity-dependent switch of the combiner. If the polarizations of the two PCs are set appropriately, the transmission of the combined light decreases when the input intensity to the SOA increases, thus suppressing the mode competition for multiwavelength generation.

4. Opto-VLSI processor

Because the limitations of the available underlying tuning mechanisms, current tunable multiwavelength lasers have very poor performances in tunability (can only shift all the wavelength channels over a very narrow wavelength range), flexibility (cannot independently control each wavelength channel), and operation ranges (limited to a single wavelengthrange). Furthermore, the flexibility limitation of conventional wavelength selection mechanisms has prevented researchers from fully understanding the mechanism of multiwavelength lasing in fibre lasers. As a result multiwavelength lasers tend to suffer from poor output power and wavelength stability. Therefore, both the wavelength selection (or tuning) mechanism and the mechanism of multiwavelength lasing are still in intensive investigation.

Advanced Opto-VLSI technology can be incorporated into a novel tuning approach, for the first time ever, to remove all previous disadvantages, thus simultaneously allowing (i) independent tuning of each wavelength channel, (ii) arbitrary control of the power level for each wavelength channel, (iii) the addition and removal of any lasing wavelength without affecting the power levels of other lasing wavelengths, and (iv) the generation of wavelength channels over various operation ranges, where each range may have output at several bands, all achieving (v) sufficient maximum continuous wave power output per channel (>+10dBm), (vi) sufficiently conserved linewidth (i.e. comparable to performance by Agilent of less than +/0.001nm at 1550 nm), (vii) minimal power fluctuations (i.e. ideally 0.01dB over 12 hours). These unique features are far superior to all tuning mechanisms reported in the literature to date, opening an excellent opportunity to develop a novel practical approach to multiwavelength lasing using Opto-VLSI processors.

A reconfigurable Opto-VLSI processor comprises an array of liquid crystal (LC) cells driven by a Very-Large-Scale-Integrated (VLSI) circuit that generates digital holographic diffraction gratings to steer and/or shape optical beams.

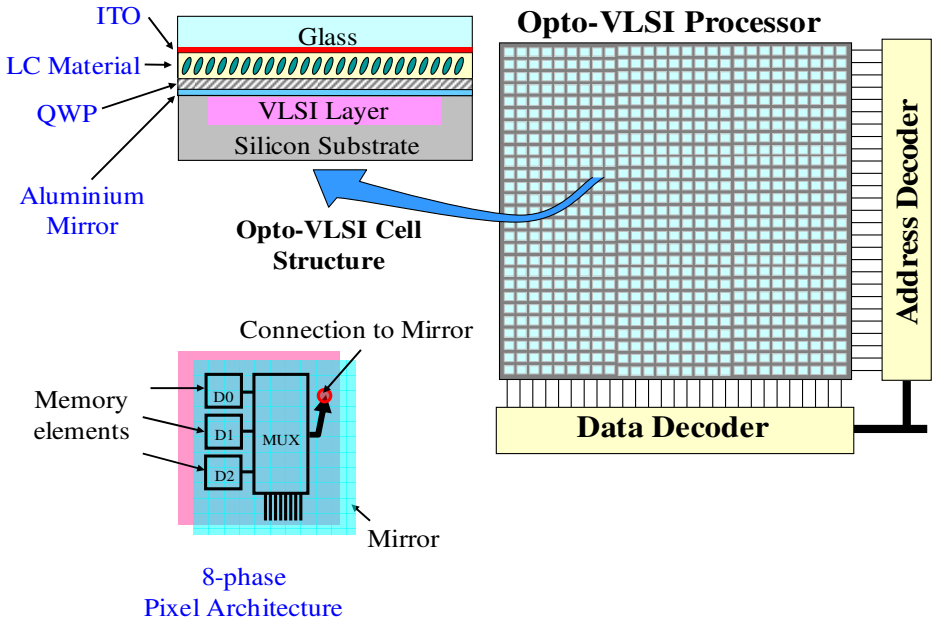

Fig. 1. Typical 8-phase Opto-VLSI processor and LC cell structure design.

Each pixel is assigned a few memory elements that store a digital value, and a multiplexer that selects one of the input voltages and applies it to the aluminium mirror plate. Opto-VLSI processors are electronically controlled, software-configured, polarization independent, cost effective because of the high-volume manufacturing capability of VLSI chips as well as the capability of controlling multiple fiber ports in one compact Opto-VLSI module, and very reliable since beam steering is achieved with no mechanically moving parts. Figure 1 shows a typical layout and a cell design of an 8-phase Opto-VLSI processor. Indium-Tin Oxide (ITO) is used as the transparent electrode, and evaporated aluminium is used as the reflective electrode. The ITO layer is generally grounded and a voltage is applied at the reflective electrode by the VLSI circuit below the LC layer.
Figure 2 illustrates the steering capability of Opto-VLSI processors. For a small incidence angle, the maximum steering angle of the Opto-VLSI processor is given by

$$\theta_{\max} = \frac{\lambda}{M \cdot d} \tag{1}$$

where M is the number of phase levels, d is the pixel size, and λ is the wavelength. For example, a 4-phase Opto-VLSI processor having a pixel size of 5 microns can steer a 1550 nm laser beam by a maximum angle of around ±4°. The maximum diffraction efficiency of an Opto-VLSI processor depends on the number of discrete phase levels that the VLSI can accommodate. The theoretical maximum diffraction efficiency is given by (Dammann, 1979)

$$\eta = \mathrm{sinc}^2\left(\frac{\pi n}{M}\right) \tag{2}$$

where $n = gM + 1$ is the diffraction order ($n = 1$ is the desired order), and g is an integer. Thus an Opto-VLSI processor with binary phase levels can have a maximum diffraction efficiency of 40.5%, while a four phase levels allow for efficiency up to 81%. The higher diffraction orders (which correspond to the cases g ≠ 0) are usually unwanted crosstalk signals, which must be attenuated or properly routed outside the output ports to maintain a high signal-to-crosstalk performance.

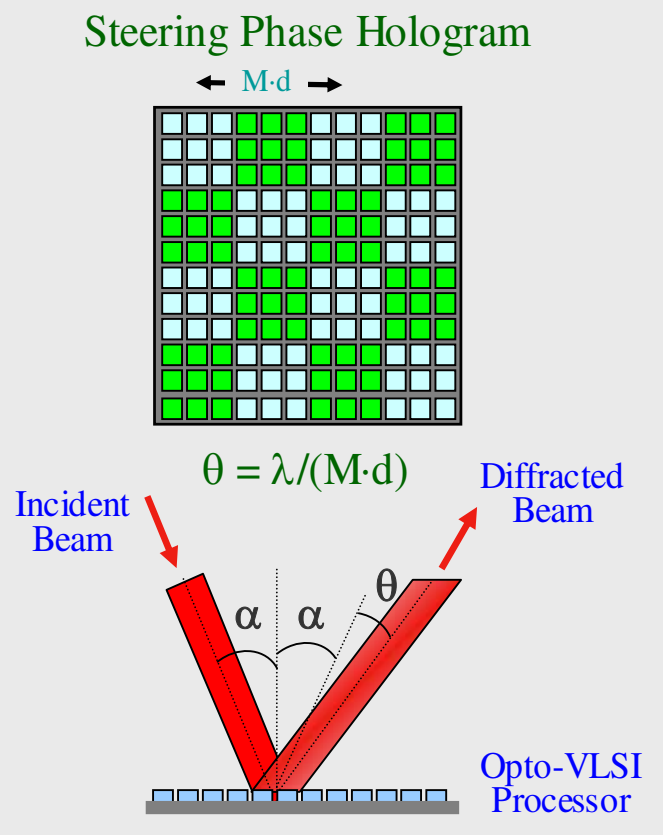

Fig. 2. Steering and multicasting capabilities of an Opto-VLSI processor.

Adaptive optical beam steering can be achieved by reconfiguring the phase hologram uploaded onto the Opto-VLSI processor. Recent advances in low-switching-voltage nematic LC materials and Layer thickness control have allowed the incorporation of a thin quarter-wave-plate (QWP) layer between the LC and the aluminium mirror to accomplish polarization-insensitive multi-phase-level Opto-VLSI processors [25], as shown in Fig. 1. In addition, with current 130nm VLSI fabrication processes, VLSI chips featuring 24mm×24mm active area, maximum switching voltage of 3.0 volts, and pixel size of 5 microns, can be realised. Depositing low-switching-voltage electro-optic materials and QWP over such VLSI chips, can realize a polarization-insensitive Opto-VLSI processor that has a diffraction efficiency of 87% (0.6 dB loss) and a maximum steering angle of more than ±4.0°.

There are several algorithms for the optimization of Opto-VLSI phase holograms to achieve effective beam steering, including simulated annealing and projection methods. In our study, a modified simulated annealing method that can achieve accurate beam steering with low crosstalk is adopted (Yen-Wei Chen *et al.*, 2000).

5. Single wavelength tunable fiber lasers

Recently, a novel tunable fiber laser employing an Opto-VLSI processor has been demonstrated (Xiao *et al.*, 2009). The Opto-VLSI processor is able to arbitrarily select narrowband optical signals from the amplified spontaneous emission (ASE) spectrum of an EDFA and inject them into a recirculating fiber ring to generate laser signals at arbitrary wavelengths. It is motionless and can be tuned electronically over the gain bandwidth of the EDFA.

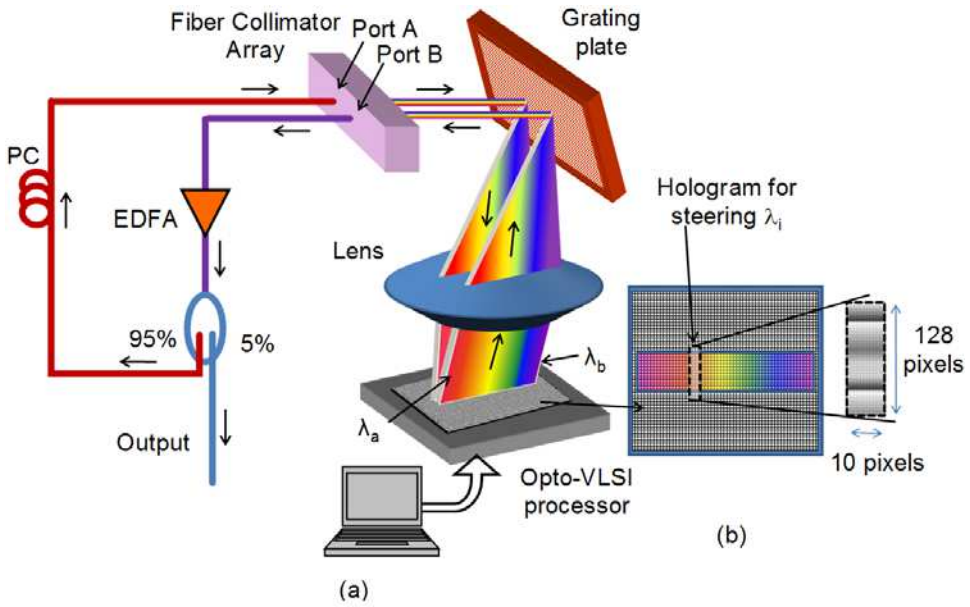

Fig. 3. Opto-VLSI-based tunable fiber laser structure.

Figure 3 shows the Opto-VLSI-based tunable fiber ring laser structure, which consists of an EDFA, an optical coupler, a polarization controller, and a fiber collimator pair (Port A and Port B). 95% of broadband ASE spectrum initially generated by the EDFA is routed to the Opto-VLSI processor through Port A of the fiber collimator array. The polarization controller (PC) is used to align the ASE polarization so that the diffraction efficiency of the Opto-VLSI processor is maximized, and also to enforce single-polarization laser operation. The grating plate demultiplexes the collimated broadband ASE signal along different directions. The lens between the Opto-VLSI processor and the grating plate has a focal length of 10 cm and is placed at 10 cm from the grating plate so that the dispersed ASE wavebands are deflected along the same direction and mapped onto the surface of an Opto-VLSI processor as illustrated in Fig. 3(a). By driving the Opto-VLSI processor with an appropriate steering phase hologram, any waveband of the ASE spectra can be routed to

and coupled into Port B of the fiber collimator array (see Fig. 3(b)), and the others are dropped out with dramatic attenuation. The selected wavebands that are coupled into Port B are amplified by the EDFA, leading, after several recirculations, to single-mode laser generation. Therefore, the fiber laser can be tuned by simply uploading appropriate phase holograms that drive the various pixels of the Opto-VLSI processor.

In the experiments, the EDFA was a C-band amplifier having a small signal gain of 14 dB, and a gain spectrum shown in Fig. 4.The EDFA's pump laser was driven with a current of 400 mA. A 256-phase-level 512×512-pixel Opto-VLSI processor of pixel size 15 μm with an insertion loss of about 0.5 dB was used. The spacing between the fiber collimator elements (Port A and Port B) was 3 mm, and the insertion loss and return loss for the two ports were 0.6 dB and 55 dB, respectively. An optical spectrum analyzer with 0.01 nm resolution was used to monitor the laser output power generated at the 5% output port of the optical coupler. The ASE signal was collimated at 0.5 mm diameter, and a blazed grating plate, having 1200 lines/mm and a blazed angle of 70° at 1530 nm, was used to demultiplex the ASE signal and map onto the active window of the Opto-VLSI processor through a lens of focal length 10 cm placed at 10 cm from the grating plate. A Labview software was developed to generate the optimized digital holograms that steer the desired waveband and couple into the collimator Port B.

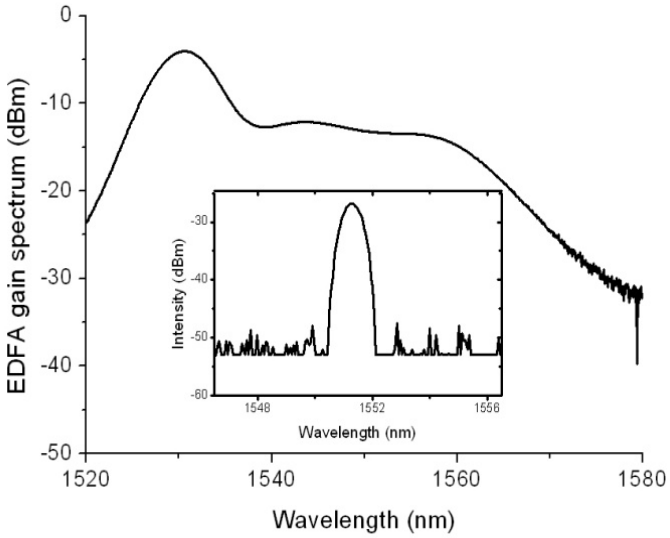

Fig. 4. Amplified spontaneous emission (ASE) noise from the EDFA. The inset is an example of a waveband selected by the Opto-VLSI processor.

When the optical loop was open, the ASE noise signal of the EDFA is shown in Fig. 4. The gain spectrum of the EDFA was linearly mapped along the active window of the Opto-VLSI processor. The inset of Fig. 4 is an example that illustrates the selection and coupling of an arbitrary waveband into Port B by uploading a phase hologram onto the Opto-VLSI processor. The measured total insertion loss from Port A to Port B was around 12 dB, which was mainly due to (i) the lens reflection loss; (ii) the blazed grating loss; and (iii) diffraction loss and insertion loss of the Opto-VLSI processor.

After the optical loop was closed, the Opto-VLSI processor was driven by different phase holograms, each corresponding to a single-mode lasing at a specific wavelength. Each selected waveband experienced a high gain by the EDFA in comparison to the gains experienced by the other ASE wavebands. Figure 5(a) shows the measured outputs of the Opto-VLSI-based fiber laser and demonstrates an excellent tuning capability over the C-band through the generation of 8×512 phase holograms at different position along the active window of the Opto-VLSI processor. The linewidth of the tunable laser was about 0.05 nm, compared to 0.5 nm when the optical loop was open (see the inset in Fig. 4). The measured side-mode suppression ratio (SMSR) was greater than 35 dB and the output power ripple was less than 0.25 dB over the entire C-band. The small ripples in the laser output power levels can be attributed to two main reasons, namely, (i) the EDFA worked in deep saturation, which clips the lasing output power; and (ii) the excellent stability and uniformity of the Opto-VLSI processor in steering and selecting wavebands over the whole C-band.

Figure 5(b) shows the measured laser outputs when fine wavelength tuning was performed by shifting the center of the phase hologram by a single pixel across the active window of the Opto-VLSI processor. The wavelength tuning step was around 0.05 nm. This corresponds to the mapping of 30 nm bandwidth of ASE spectrum of the EDFA across the 512 pixels (each of 15 μm size). Note that the tuning resolution can be made smaller by using an Opto-VLSI processor with a smaller pixel size. Note that the shoulders on both sides of the laser spectrum may be due to self-phase modulation or other nonlinear phenomena arising from a high-level of the output power.

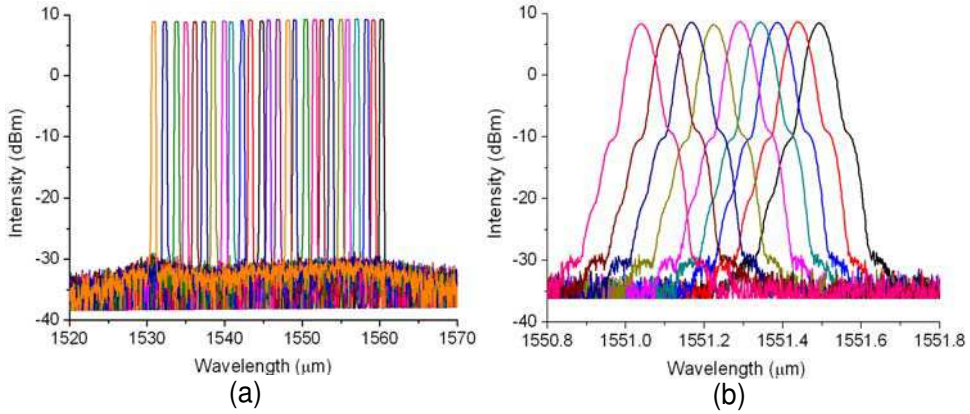

Fig. 5. Measured output intensities of the Opto-VLSI-based fiber laser，(a) Coarse wavelength tuning over C-band, and (b) fine wavelength tuning.

The measured crosstalk between Port A to Port B, defined as the ratio of the unselected ASE signal to the power of the waveband selected by the Opto-VLSI processor, was less than -55 dB. This crosstalk level, which contributes to the background level of the laser output and SMSR, can further be reduced by (i) increasing the spacing between Port A and Port B, (ii) improving the imaging quality of the lens, (iii) increasing the collimated beam diameter, and (iv) reducing the pixel size of the Opto-VLSI processor. The laser exhibited very stable operation at room temperature when it was turned on for different periods of time ranging from a few hours to a few days.

6. Multiple wavelength tunable fiber lasers

Beside its flexible single-wavelength tunable capability, Opto-VLSI processor is also able to offer super multi-wavelength tunability. Furthermore, this tuning mechanism provides two advanced features which cannot be provided by other tuning mechanisms, namely, (i) any of the lasing wavelengths can be tuned simultaneously and independently; (ii) any wavelength channel can be switched on/off without affecting the other wavelength channels, adding an important new function to the current tunable multiwavelength fiber lasers. These novel functions are very attractive for many applications such as optical telecommunications, optical characterization and testing, photonic RF signal processing.

The structure for the Opto-VLSI-based tunable multiwavelength fiber ring laser is the same as the one shown in Fig. 3, with the only difference that an SOA is inserted into the laser cavity to construct a hybrid gain medium which provides stable multiwavelength lasing. By driving the Opto-VLSI processor with an appropriate steering phase hologram, multiple wavebands from the ASE spectra can be steered and coupled into Port 2 of the fiber collimator array, and the others are dropped out with dramatic attenuation. The selected wavebands that are coupled into Port 2 are amplified by the EDFA and SOA, thus forming an optical loop for multiwavelength laser generation. In this way, the fiber laser can be tuned by simply uploading appropriate steering phase holograms that drive the various pixels of the Opto-VLSI processor. The Opto-VLSI-based tunable multiwavelength fiber laser shown in Fig. 3 is able to tune multiple lasers simultaneously and independently. This architecture offers excellent non-inertial tuning flexibility because any waveband within the ASE spectra from the gain media can independently be selected using computer generated holograms.

The principle of the Opto-VLSI-based tunable multiwavelength fiber laser is demonstrated by the experimental setup illustrated in Fig. 3. An EDFA and an SOA, both operating within the wavelength region of C-band, were driven with currents of 400 mA and 300 mA, respectively. A Labview software was specially developed to generate the optimized digital holograms that steer the desired wavebands and couple into Port 2.

Note that the output port was chosen to be immediately after the EDFA, because the homogeneous line broadening of the EDFA results in low background noise when multiple lasing wavelengths are synthesized. A tunable 5-wavelength fiber laser was generated by applying an optimized phase hologram to steer 5 associated wavebands and couple into the fiber ring. Three experimental scenarios were carried out to prove the tunability of the proposed structure, including tuning with equal wavelength spacing, tuning with arbitrary wavelength spacing, and switching on/off wavelength channels.

Figure 6 shows the results of the first scenario, where the Opto-VLSI processor was reconfigured to tune the multiwavelength laser with equal wavelength spacing. A 5-wavelength laser with equal wavelength spacing of 1.14 nm were firstly synthesized using a phase hologram optimized in such a way that the pixel blocks associated with the 5 wavelength channels are uploaded with steering blazed gratings that appropriately steer and couple these channels back into the fiber ring while the other wavelength channels are not steered, thus experiencing dramatic coupling losses. The wavelength spacing of the 5-wavelength laser was tuned from 1.14 nm to 1.68 nm, then 2.22 nm by reconfiguring the phase hologram. The output power for each laser channel was around +6 dBm and the SMSR was better than 30 dB. The laser linewidth was about 0.4 nm, and the power uniformity was less than 0.8 dB. This small measured power uniformity is attributed to the fact that the intensity of each wavelength channel in the cavity can be arbitrarily controlled

by adjusting the steering efficiency of the various pixel blocks associated to the lasing channels. In addition, the relatively high laser output power was because of the low insertion loss experienced by each wavelength channel.

The measured minimum wavelength spacing of the multiwavelength laser was around 0.4 nm, which is determined by the pixel size of the Opto-VLSI processor, the focal length of the lens, and the dispersion capability of the grating plate. In the experiments, the 30 nm ASE spectrum was mapped across the 512-pixel surface of the Opto-VLSI processor (each of 15 um size), thus each pixel was occupied by about 0.05 nm of the tuning range, and 8x512-pixel pixel blocks were used to steer the individual wavelength channels, resulting in 0.4 nm channel linewidth (and hence minimum channel spacing), and 0.05 nm tuning resolution for each wavelength channel corresponding to one pixel shift. Note that the wavelength spacing and the tuning resolution can be made smaller by using an Opto-VLSI processor with a smaller pixel size and a larger active window.

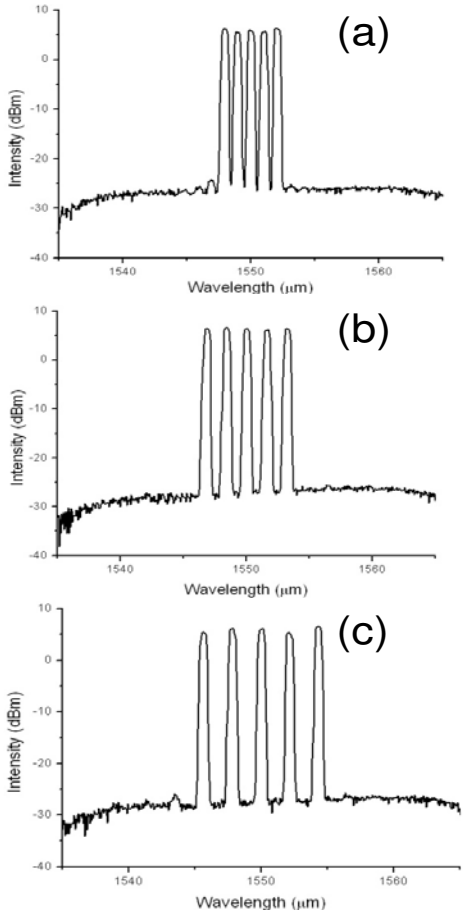

Fig. 6. Tuning with equal wavelength spacing for the Opto-VLSI-based tunable multiwavelength fiber laser.

The second scenario demonstrated that the wavelength spacing of the multiwavelength laser can arbitrary be tuned, as shown in Fig. 7. Starting from the 1.14nm spaced wavelength channels shown in Fig. 6(a), the adjacent wavelength spacings were changed to [1.14 nm, 1.14nm, 1.68 nm, 1.68 nm] as shown in Fig. 7(a). This was accomplished by shifting the steering phase holograms associated to the fourth and fifth wavelength channels by 10 pixels. Similarly, the adjacent wavelength spacing was tuned to [1.14 nm, 1.68nm, 1.68 nm, 1.68 nm] and [1.68 nm, 1.68nm, 1.68 nm, 2.22 nm] as shown in Figs. 7(b) and (c), respectively. Note that when the wavelength spacing of the multiwavelength laser was varied, a negligible change in the output levels for each wavelength and the output power uniformity was observed. However, the other laser characteristics such as output SMSR, laser linewidth, tuning step, did not change.

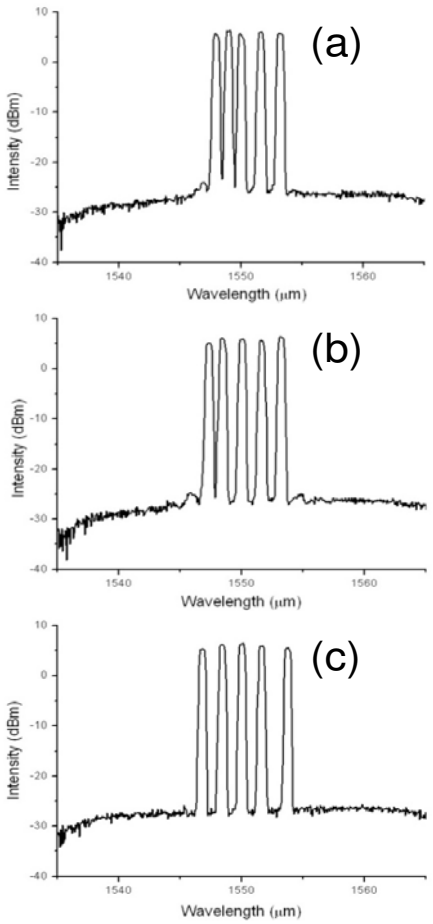

Fig. 7. Tuning with arbitrary wavelength spacing for the Opto-VLSI-based tunable multiwavelength fiber laser.

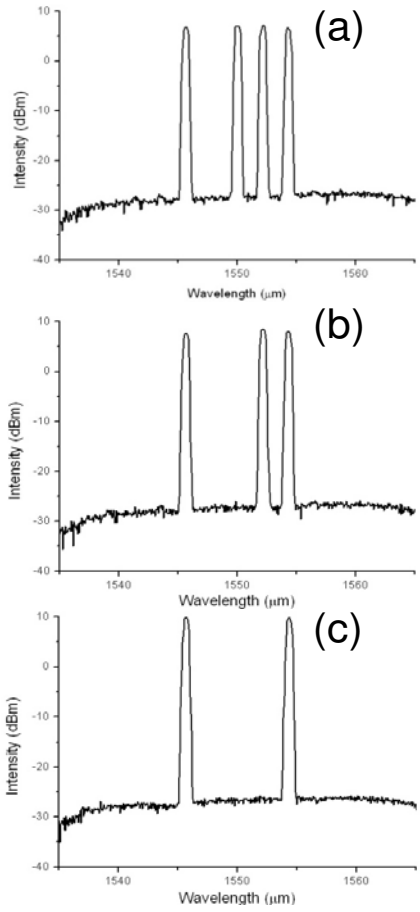

Fig. 8. Switching on/off any wavelength channels.

In the third scenario, we demonstrated that each wavelength channel can independently be switched on/off. Starting from the multiwavelength laser output shown in Fig. 7(c), and by removing the steering phase hologram associated to the second wavelength channel, the latter was switched off and dropped out from the fiber ring while the other channels were kept intact, as shown in Fig. 8(a). Similarly, the third and the fourth wavelength channels were dropped, as illustrated in Figs. 8(b) and (c), by reconfiguring the phase hologram uploaded onto the Opto-VLSI processor. During the switching experiments, the multiwavelength laser characteristics such as the output power level, the power uniformity, laser linewidth, and SMSR were not affected.

The above three scenarios demonstrate the capability of the multiwavelength laser to generate arbitrary wavelength channels via software, leading to significant improvement in flexibility and reconfigurability compared to previously reported tunable multiwavelength laser demonstrators.

Each wavelength channel exhibited very stable operation at room temperature whenever it was turned on for different periods of time ranging from a few hours to a few days. The measured maximum output power fluctuation was less than 0.5 dB for a period of 2-hour observation.

7. Multi-port tunable fiber lasers

In addition to its excellent tunability for both single-wavelength and multi-wavelength lasing, the Opto-VLSI based approach provides a special capability of integrating many tunable single/multi-wavelength fiber lasers into a same tuning system, making it very competitive for commercialization.

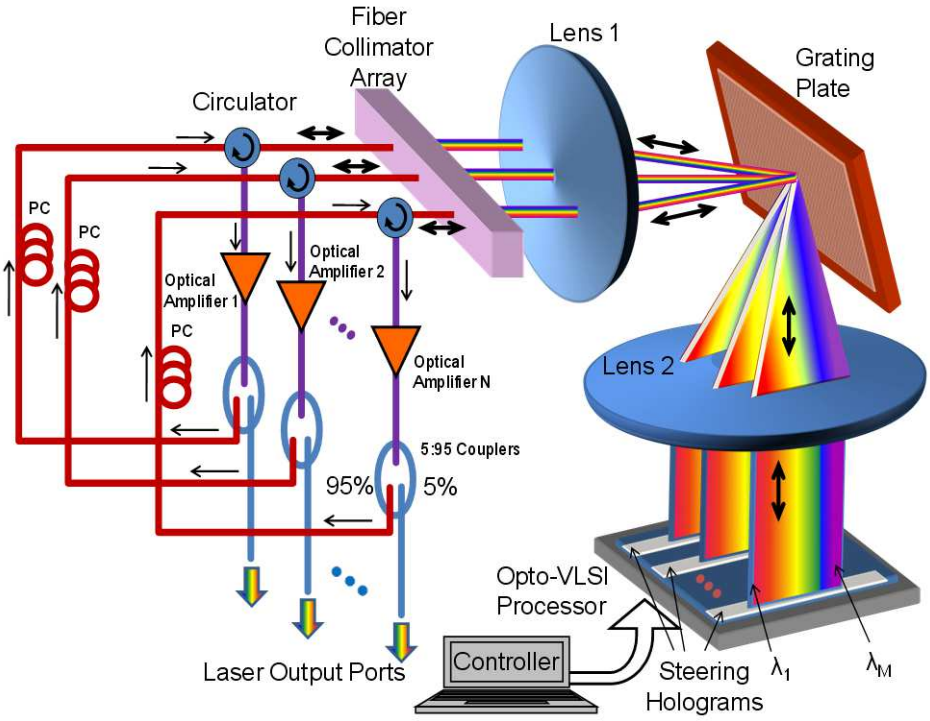

Fig. 9. The proposed multi-port tunable fiber laser structure.

The proposed Opto-VLSI-based multi-port tunable fiber ring laser structure is shown in Fig. 9. It consists of N tunable fiber lasers simultaneously driven by a single Opto-VLSI processor. Each tunable fiber laser employs an optical amplifier, an optical coupler, a polarization controller, a circulator, and one port from a collimator array, as described in Fig. 9. All the broadband ASE signals are directed to the corresponding collimator ports, via their corresponding circulators. A lens (Lens 1) is used between the collimator array and a diffraction grating plate to focus the collimated ASE beams onto a small spot onto the grating plate. The latter demultiplexes all the collimated ASE signals into wavebands (of different center wavelengths) along different directions. Another lens (Lens 2), located in the

middle position between the grating plate and the Opto-VLSI processor, is used to collimate the dispersed optical beams in two dimensions and map them onto the surface of a 2-D Opto-VLSI processor, which is partitioned into N rectangular pixel blocks. Each pixel block is assigned to a tunable laser and used to efficiently couple back any part of the ASE spectrum illuminating this pixel block along the incident path into the corresponding collimator port. The selected waveband coupled back into the fiber collimator port is then routed back to the gain medium via the corresponding circulator, thus an optical loop is formed for the single-mode laser generation. Therefore, by uploading the appropriate phase holograms (or blazed grating) that drive all the pixel blocks of the Opto-VLSI processor, N different wavelengths can independently be selected for lasing within the different fiber loops, thus realizing a multiport tunable fiber laser source that can simultaneously generate arbitrary wavelengths at its ports. Note that the N tunable fiber lasers can independent and simultaneously offer lasing in sing wavelength, multi wavelength, or hybrid.

To proof the principle of the proposed Opto-VLSI-based tunable fiber laser, an Opto-VLSI-based 3-wavelength tunable fiber laser was demonstrated using the experimental setup shown in Fig. 9. Each tunable fiber laser channel consists of an EDFA that operates in the C-band, a 1×2 optical coupler with 5/95 power splitting ratio, and a fiber collimator array. A 256-phase-level two-dimensional Opto-VLSI processor having 512×512 pixels with 15 μm pixel size was used to independently and simultaneously select any part of the gain spectrum from each EDFA into the corresponding fiber ring. Two identical lenses of focal length 10 cm were placed at 10 cm from both sides of the grating plate. An optical spectrum analyzer with 0.01 nm resolution was used to monitor the 5% output port of each optical coupler which serves as the output port for each tunable laser channel. The 95% port of each ASE signal was directed to a PC and collimated at about 0.5 mm diameter. A blazed grating, having 1200 lines/mm and a blazed angle of 70º at 1530 nm, was used to demultiplex the three EDFA gain spectra, which were mapped onto the active window of the Opto-VLSI processor by Lens 2. A Labview software was especially developed to generate the optimized digital holograms that steer the desired waveband and couple back into the corresponding collimator for subsequent recirculation in the fiber loop.

The active window of the Opto-VLSI processor was divided into three pixel blocks corresponding to the positions of the three demultiplexed ASE signals, each pixel block dedicated for tuning the wavelength of a fiber laser. Optimized digital phase holograms were applied to the three pixel blocks, so that desired wavebands from the ASE spectra illuminating the Opto-VLSI processor could be selected and coupled back into their fiber rings, leading to simultaneous lasing at specific wavelengths. By changing the position of the phase hologram of each pixel block, the lasing wavelength for each fiber laser could be dynamically and independently tuned. The measured total cavity loss for each channel was around 12 dB, which mainly includes (i) the coupling loss of the associated collimator; (ii) the blazed grating loss; and (iii) the diffraction loss and insertion loss of the Opto-VLSI processor. Note that the total cavity loss influences both the laser output power and the tuning range, as well as the pump current thresholds needed for lasing (60mA in the experiments).

Figure 10 demonstrates the coarse tuning capability of the 3-wavelength Opto-VLSI fiber laser operating over C-band. The measured output laser spectrum for each channel is shown for different optimized phase holograms uploaded onto the Opto-VLSI processor. All the channels could independently and simultaneously be tuned over the whole C-band. Port 1 and Port 2 have an output power level of about 9 dBm with an optical side-mode-suppression-ratio of more than 35 dB. Port 3 has 2 dB less output power because the EDFA's

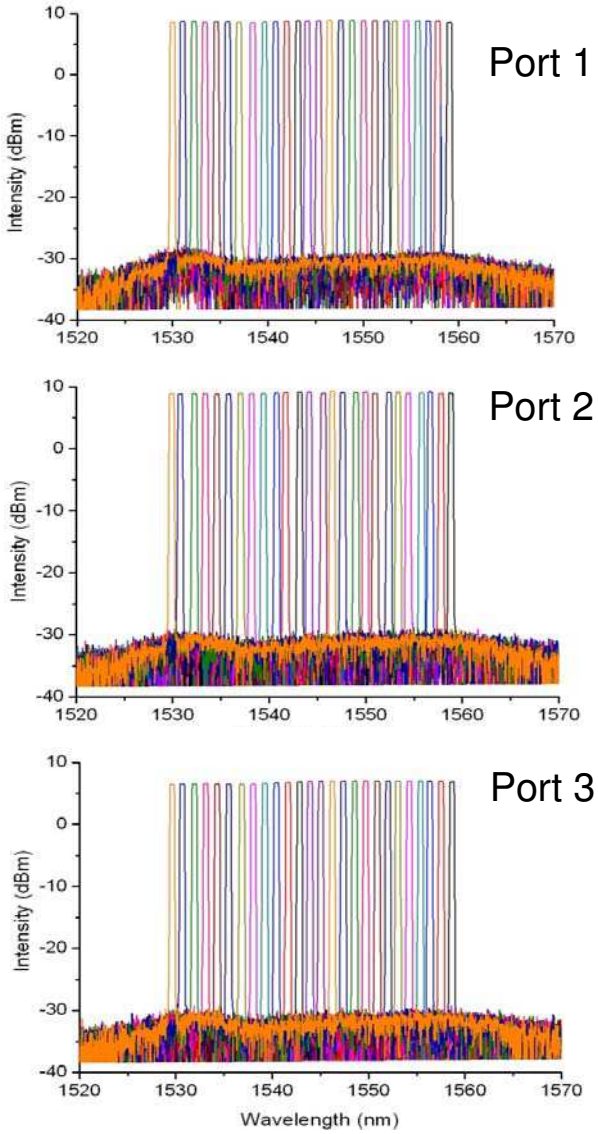

Fig. 10. Measured responses of the Opto-VLSI-based 3-wavelength fiber laser for coarse tuning operation over C-band. These three channels can independently and simultaneously be tuned over the whole C-band.

gain for this channel was intentionally dropped to demonstrate the ability to change the output power level via changing the pump current. The laser output power for each channel has a uniformity of about 0.5 dB over the whole tuning range. Each laser channel exhibited the same performance as described before when only one fiber laser is constructed based on the Opto-VLSI processor.

The maximum output power for the multi-wavelength tunable fiber laser is about 9 dBm. This value is mainly dependent on the gain of the EDFA associated to that channel. Note that the thickness of the liquid crystal layer of the Opto-VLSI processor is very small (several microns), leading to spatial phase-modulation with negligible power loss. For high laser output power levels, the nonlinearity of the LC material could induce unequal phase shifts to the individual pixels of the steering phase hologram, leading to higher coupling loss, which reduces the output laser power. However, properly designed liquid-crystal mixtures can handle optical intensities as high as 700 W/cm2 with negligible nonlinear effects, making the maximum laser output power mainly dependent on the maximum output optical power of the gain medium.

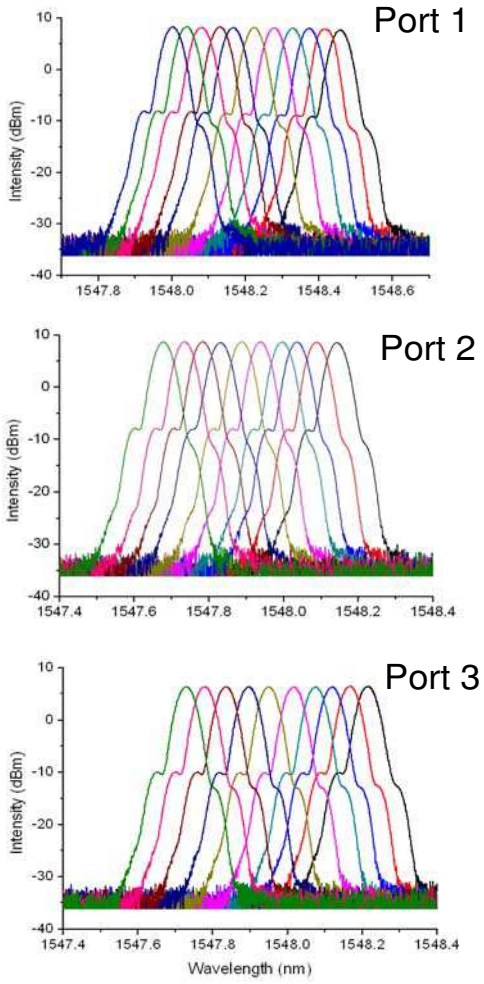

Fig. 11. Fine tuning operation for each channel of the Opto-VLSI-based 3-wavelength tunable fiber laser. The minimum tuning step was 0.05 nm.

The measured laser outputs for fine wavelength tuning operation of the three channels are shown in Fig. 11. By shifting the center of each phase hologram by a single pixel across the active window of the Opto-VLSI processor, the wavelength was tuned by a step of around 0.05 nm for all the three channels. This corresponds to the mapping of 30 nm ASE spectrum of the EDFA of each channel across the 512 pixels (each of 15 μm size). Similarly, the shoulders on both sides of the laser spectrum of each tunable laser channel are due to self-phase modulation or other nonlinear phenomena arising from a high level of the output power, as also shown in Fig. 11(b).

When the output power of each fiber laser is varied via the control of the current driving the pump laser of the EDFA, the other laser characteristics such as output SMSR, laser linewidth, output power uniformity, tuning step, and tuning range were not changed. The pump-independent laser linewidth observation might be due to the limited resolution (0.01 nm) of the OSA we used in the experiments.

Since the Opto-VLSI processor has a broad spectral bandwidth, the multi-port tunable laser structure shown in Fig. 9 could in principle operate over the O-, S-, C- and/or L- bands. Note also that the Opto-VLSI processor used in the experiment was able to achieve wavelength tuning for up to 8 ports independently and simultaneously. This is because each pixel block was about 0.8 mm wide and the active window of the Opto-VLSI active window was 7.6 mm × 7.6 mm.

8. Conclusion

In this chapter, the tuning mechanisms and gain mechanisms for single-wavelength, multi-wavelength tunable fiber lasers have been reviewed. Then the use of optical amplifiers and Opto-VLSI technology to realize a tunable single/multiple wavelength fiber laser and multi-port tunable fiber lasers, has been discussed. The ability of the Opto-VLSI processor to select any part of the gain spectrum from optical amplifiers into desired fiber rings has been demonstrated, leading to many tunable single/multiple wavelength fiber laser sources. We have also experimentally demonstrated the proof-of-principle of tunable fiber lasers capable of generating single and/or multiple wavelengths laser sources with laser linewidth as narrow as 0.05 nm, optical side-mode-suppression-ratio (SMSR) of about 35 dB, as well as outstanding tunability. The demonstrated tunable fiber lasers have excellent stability at room temperature and output power uniformity less than 0.5 dB over the whole C-band. In addition, this tunable fiber laser structure could potentially operate over the O-, S-, C- and/or L- bands.

9. Acknowledgement

We acknowledge the support of the Department of Nano-bio Materials and Electronics, Gwangju Institute of Science and Technology, Republic of Korea, for the development of the tunable laser demonstrator.

10. References

Alvarez-Chavez, J. A., Martinez-Rios, A., Torres-Gomez, I. & Offerhaus, H. L. (2007). Wide wavelength-tuning of a double-clad Yb3+-doped fiber laser based on a fiber Bragg grating array. Laser Physics Letters, Vol. 4, No. 12, pp. 880-883, Issn: 1612-2011.

Belanger, E., Bernier, M., Faucher, D., Cote, D. & Vallee, R. (2008). High-power and widely tunable all-fiber Raman laser. Journal of Lightwave Technology, Vol. 26, No. 9-12, pp. 1696-1701, Issn: 0733-8724.

Bellemare, A. (2003). Continuous-wave silica-based erbium-doped fibre lasers. Progress in Quantum Electronics, Vol. 27, pp. 211-266

Bellemare, A., Karasek, M., Riviere, C., Babin, F., He, G., Roy, V. & Schinn, G. W. (2001). A broadly tunable erbium-doped fiber ring laser: experimentation and modeling. Ieee Journal of Selected Topics in Quantum Electronics, Vol. 7, No. 1, pp. 22-29, Issn: 1077-260X.

Bellemare, A., Karasek, M., Rochette, M., LaRochelle, S. & Tetu, M. (2000). Room temperature multifrequency erbium-doped fiber lasers anchored on the ITU frequency grid. Journal of Lightwave Technology, Vol. 18, No. 6, pp. 825-831, Issn: 0733-8724.

Chang, S. H., Hwang, I. K., Kim, B. Y. & Park, H. G. (2001). Widely tunable single-frequency Er-doped fiber laser with long linear cavity. Ieee Photonics Technology Letters, Vol. 13, No. 4, pp. 287-289, Issn: 1041-1135.

Chen, D. R., Qin, S. & He, S. L. (2007). Channel-spacing-tunable multi-wavelength fiber ring laser with hybrid Raman and erbium-doped fiber gains. Optics Express, Vol. 15, pp. 930-935, Issn: 1094-4087.

Chen, H. X. (2005). Multiwavelength fiber ring lasing by use of a semiconductor optical amplifier. Optics Letters, Vol. 30, No. 6, pp. 619-621, Issn: 0146-9592.

Chen, Y.-W., Yamauchi, S., Wang, N. & Nakao, Z. (2000). A fast kinoform optimization algorithm based on simulated annealing. IEICE Trans. Fundamentals, Vol. E83-A, No. 4, pp. 3

Cheng, Y., Kringlebotn, J. T., Loh, W. H., Laming, R. I. & Payne, D. N. (1995). STABLE SINGLE-FREQUENCY TRAVELING-WAVE FIBER LOOP LASER WITH INTEGRAL SATURABLE-ABSORBER-BASED TRACKING NARROW-BAND-FILTER. Optics Letters, Vol. 20, No. 8, pp. 875-877, Issn: 0146-9592.

Chien, H. C., Yeh, C. H., Lai, K. H., Lee, C. C. & Chi, S. (2005a). Stable and wavelength-tunable erbium-doped fiber double-ring laser in S-band window operation. Optics Communications, Vol. 249, No. 1-3, pp. 261-264, Issn: 0030-4018.

Chien, H. C., Yeh, C. H., Lee, C. C. & Chi, S. (2005b). A tunable and single-frequency S-band erbium fiber laser with saturable-absorber-based autotracking filter. Optics Communications, Vol. 250, No. 1-3, pp. 163-167, Issn: 0030-4018.

Chow, K. K., Shu, C., Mak, M. & Tsang, H. K. (2002). Widely tunable wavelength converter using a double-ring fiber laser with a semiconductor optical amplifier. Ieee Photonics Technology Letters, Vol. 14, No. 10, pp. 1445-1447, Issn: 1041-1135.

Dammann, H. (1979). Spectral characteristics of stepped-phase gratings. Optik, Vol. 53 pp. 9

Das, G. & Lit, J. W. Y. (2002). L-band multiwavelength fiber laser using an elliptical fiber. Ieee Photonics Technology Letters, Vol. 14, No. 5, pp. 606-608, Issn: 1041-1135.

Dong, H., Zhu, G., Wang, Q., Sun, H., Dutta, N. K., Jaques, J. & Piccirilli, A. B. (2005a). Multiwavelength fiber ring laser source based on a delayed interferometer. Ieee Photonics Technology Letters, Vol. 17, No. 2, pp. 303-305, Issn: 1041-1135.

Dong, X. Y., Ngo, N. Q., Shum, P. & Tam, H. Y. (2003). Linear cavity erbium-doped fiber laser with over 100 nm tuning range. Optics Express, Vol. 11, No. 14, pp. 1689-1694, Issn: 1094-4087.

Dong, X. Y., Shum, P., Ngo, N. Q. & Chan, C. C. (2006). Multiwavelength Raman fiber laser with a continuously-tunable spacing. Optics Express, Vol. 14, No. 8, pp. 3288-3293, Issn: 1094-4087.

Dong, X. Y., Shum, P., Ngo, N. Q. & Tam, H. Y. (2005b). Output power characteristics of tunable erbium-doped fiber ring lasers. Journal of Lightwave Technology, Vol. 23, No. 3, pp. 1334-1341, Issn: 0733-8724.

Fok, M. P., Lee, K. L. & Shu, C. (2005). Waveband-switchable SOA ring laser constructed with a phase modulator loop mirror filter. Ieee Photonics Technology Letters, Vol. 17, No. 7, pp. 1393-1395, Issn: 1041-1135.

Fu, Z. H., Yang, D. Z., Ye, W., Kong, J. & Shen, Y. H. (2009). Widely tunable compact erbium-doped fiber ring laser for fiber-optic sensing applications. Optics and Laser Technology, Vol. 41, No. 4, pp. 392-396, Issn: 0030-3992.

Han, Y. G., Dong, X. Y., Kim, C. S., Jeong, M. Y. & Lee, J. H. (2007). Flexible all fiber Fabry-Perot filters based on superimposed chirped fiber Bragg gratings with continuous FSR tunability and its application to a multiwavelength fiber laser. Optics Express, Vol. 15, No. 6, pp. 2921-2926, Issn: 1094-4087.

Han, Y. G., Kim, G., Lee, J. H., Kim, S. H. & Lee, S. B. (2005). Lasing wavelength and spacing switchable multiwavelength fiber laser from 1510 to 1620 nm. Ieee Photonics Technology Letters, Vol. 17, No. 5, pp. 989-991, Issn: 1041-1135.

Han, Y. G., Tran, T. V. A. & Lee, S. B. (2006). Wavelength-spacing tunable multi wavelength erbium-doped fiber laser based on four-wave mixing of dispersion-shifted fiber. Optics Letters, Vol. 31, No. 6, pp. 697-699, Issn: 0146-9592.

Kang, M. S., Lee, M. S., Yong, J. C. & Kim, B. Y. (2006). Characterization of wavelength-tunable single-frequency fiber laser employing acoustooptic tunable filter. Journal of Lightwave Technology, Vol. 24, No. 4, pp. 1812-1823, Issn: 0733-8724.

Kim, C. S., Sova, R. M. & Kang, J. U. (2003). Tunable multi-wavelength all-fiber Raman source using fiber Sagnac loop filter. Optics Communications, Vol. 218, No. 4-6, pp. 291-295, Issn: 0030-4018.

Lee, C. C., Chen, Y. K. & Liaw, S. K. (1998). Single-longitudinal-mode fiber laser with a passive multiple-ring cavity and its application for video transmission. Optics Letters, Vol. 23, No. 5, pp. 358-360

Lee, K. L., Fok, M. P., Wan, S. M. & Shu, C. (2004). Optically controlled Sagnac loop comb filter. Optics Express, Vol. 12, No. 25, pp. 6335-6340

Li, S. Y., Ngo, N. Q. & Zhang, Z. R. (2008). Tunable Fiber Laser With Ultra-Narrow Linewidth Using A Tunable Phase-Shifted Chirped Fiber Grating. Ieee Photonics Technology Letters, Vol. 20, No. 17-20, pp. 1482-1484, Issn: 1041-1135.

Liaw, S. K., Hung, K. L., Lin, Y. T., Chiang, C. C. & Shin, C. S. (2007). C-band continuously tunable lasers using tunable fiber Bragg gratings. Optics and Laser Technology, Vol. 39, No. 6, pp. 1214-1217, Issn: 0030-3992.

Liu, H. L., Tam, H. Y., Chung, W. H., Wai, P. & Sugimoto, N. (2005a). La-codoped bismuth-based erbium-doped fiber ring laser, with 106-nm tuning range. Ieee Photonics Technology Letters, Vol. 17, No. 2, pp. 297-299, Issn: 1041-1135.

Liu, H. L., Tam, H. Y., Chung, W. H., Wai, P. & Sugimoto, N. (2006). Low beat-noise polarized tunable fiber ring laser. Ieee Photonics Technology Letters, Vol. 18, No. 5-8, pp. 706-708, Issn: 1041-1135.

Liu, X. M., Zhou, X. Q., Tang, X. F., Ng, J., Hao, J. Z., Chai, T. Y., Leong, E. & Lu, C. (2005b). Switchable and tunable multiwavelength erbium-doped fiber laser with fiber bragg gratings and photonic crystal fiber. Ieee Photonics Technology Letters, Vol. 17, No. 8, pp. 1626-1628, Issn: 1041-1135.

Liu, Z. Y., Liu, Y. G., Du, J. B., Kai, G. Y. & Dong, X. Y. (2008). Tunable multiwavelength erbium-doped fiber laser with a polarization-maintaining photonic crystal fiber Sagnac loop filter. Laser Physics Letters, Vol. 5, No. 6, pp. 446-448, Issn: 1612-2011.

Luo, A. P., Luo, Z. C. & Xu, W. C. (2009). Tunable and switchable multiwavelength erbium-doped fiber ring laser based on a modified dual-pass Mach-Zehnder interferometer. Optics Letters, Vol. 34, No. 14, pp. 2135-2137, Issn: 0146-9592.

MOLLIER, P., ARMBRUSTER, V., PORTE, H. & GOEDGEBUER, J. P. (1995). ELECTRICALLY TUNABLE ND3+-DOPED FIBER LASER USING NEMATIC LIQUID-CRYSTALS. Electronics Letters, Vol. 31, No. 15, pp. 1248-1250, Issn: 0013-5194.

Moon, D. S., Kim, B. H., Lin, A. X., Sun, G. Y., Han, W. T., Han, Y. G. & Chung, Y. (2007). Tunable multi-wavelength SOA fiber laser based on a Sagnac loop mirror using an elliptical core side-hole fiber. Optics Express, Vol. 15, No. 13, pp. 8371-8376, Issn: 1094-4087.

Moon, D. S., Paek, U. C., Chung, Y. J., Dong, X. Y. & Shum, P. (2005). Multi-wavelength linear-cavity tunable fiber laser using a chirped fiber Bragg grating and a few-mode fiber Bragg grating. Optics Express, Vol. 13, No. 15, pp. 5614-5620, Issn: 1094-4087.

Nasir, M., Yusoff, Z., Al-Mansoori, M. H., Rashid, H. & Choudhury, P. K. (2009). Widely tunable multi-wavelength Brillouin-erbium fiber laser utilizing low SBS threshold photonic crystal fiber. Optics Express, Vol. 17, No. 15, pp. 12829-12834, Issn: 1094-4087.

Ohara, S. & Sugimoto, N. (2008). Bi2O3-based erbium-doped fiber laser with a tunable range over 130 nm. Optics Letters, Vol. 33, No. 11, pp. 1201-1203, Issn: 0146-9592.

Park, N., Dawson, J. W., Vahala, K. J. & Miller, C. (1991). All fiber, low threshold, widely tunable single-frequency, erbium-doped fiber ring laser with a tandem fiber Fabry-Perot filter. Applied Physics Letters, Vol. 59, pp. 2369-2371

Pleros, N., Bintjas, C., Kalyvas, M., Theophilopoulos, G., Yiannopoulos, K., Sygletos, S. & Avramopoulos, H. (2002). Multiwavelength and power equalized SOA laser sources. Ieee Photonics Technology Letters, Vol. 14, No. 5, pp. 693-695, Issn: 1041-1135.

Poustie, A. J., Finlayson, N. & Harper, P. (1994). MULTIWAVELENGTH FIBER LASER USING A SPATIAL MODE BEATING FILTER. Optics Letters, Vol. 19, No. 10, pp. 716-718, Issn: 0146-9592.

Qian, J. R., Su, J. & Hong, L. (2008). A widely tunable dual-wavelength erbium-doped fiber ring laser operating in single longitudinal mode. Optics Communications, Vol. 281, No. 17, pp. 4432-4434, Issn: 0030-4018.

Roy, V., Piche, M., Babin, F. & Schinn, G. W. (2005). Nonlinear wave mixing in a multilongitudinal-mode erbium-doped fiber laser. Optics Express, Vol. 13, No. 18, pp. 6791-6797, Issn: 1094-4087.

Sakata, H., Yoshimi, H. & Otake, Y. (2009). Wavelength tunability of L-band fiber ring lasers using mechanically induced long-period fiber gratings. Optics Communications, Vol. 282, No. 6, pp. 1179-1182, Issn: 0030-4018.

Song, Y. W., Havstad, S. A., Starodubov, D., Xie, Y., Willner, A. E. & Feinberg, J. (2001). 40-nm-wide tunable fiber ring laser with single-mode operation using a highly stretchable FBG. Ieee Photonics Technology Letters, Vol. 13, No. 11, pp. 1167-1169, Issn: 1041-1135.

Sun, G. Y., Moon, D. S., Lin, A. X., Han, W. T. & Chung, Y. J. (2008). Tunable multiwavelength fiber laser using a comb filter based on erbium-ytterbium co-doped polarization maintaining fiber loop mirror. Optics Express, Vol. 16, No. 6, pp. 3652-3658, Issn: 1094-4087.

Sun, J. Q., Qiu, J. L. & Huang, D. X. (2000). Multiwavelength erbium-doped fiber lasers exploiting polarization hole burning. Optics Communications, Vol. 182, No. 1-3, pp. 193-197, Issn: 0030-4018.

Tran, T. V. A., Lee, K., Lee, S. B. & Han, Y. G. (2008). Switchable multiwavelength erbium doped fiber laser based on a nonlinear optical loop mirror incorporating multiple fiber Bragg gratings. Optics Express, Vol. 16, No. 3, pp. 1460-1465, Issn: 1094-4087.

Ummy, M. A., Madamopoulos, N., Lama, P. & Dorsinville, R. (2009). Dual Sagnac loop mirror SOA-based widely tunable dual-output port fiber laser. Optics Express, Vol. 17, No. 17, pp. 14495-14501, Issn: 1094-4087.

Xiao, F., Alameh, K. & Lee, T. (2009). Opto-VLSI-based tunable single-mode fiber laser. Optics Express, Vol. 17, No. 21, pp. 18676-18680, Issn: 1094-4087.

Xu, L., Wang, B. C., Baby, V., Glesk, I. & Prucnal, P. R. (2002). Optical spectral bistability in a semiconductor fiber ring laser through gain saturation in an SOA. Ieee Photonics Technology Letters, Vol. 14, No. 2, pp. 149-151, Issn: 1041-1135.

Yamashita, S. & Hotate, K. (1996). Multiwavelength erbium-doped fibre laser using intracavity etalon and cooled by liquid nitrogen. Electronics Letters, Vol. 32, No. 14, pp. 1298-1299, Issn: 0013-5194.

Yeh, C. H. & Chi, S. (2005). A broadband fiber ring laser technique with stable and tunable signal-frequency operation. Optics Express, Vol. 13, No. 14, pp. 5240-5244, Issn: 1094-4087.

Zhang, J. L., Yue, C. Y., Schinn, G. W., Clements, W. R. L. & Lit, J. W. Y. (1996). Stable single-mode compound-ring erbium-doped fiber laser. Journal of Lightwave Technology, Vol. 14, No. 1, pp. 104-109, Issn: 0733-8724.

Zhang, Z. X., Wu, J., Xu, K., Hong, X. B. & Lin, J. T. (2009). Tunable multiwavelength SOA fiber laser with ultra-narrow wavelength spacing based on nonlinear polarization rotation. Optics Express, Vol. 17, No. 19, pp. 17200-17205, Issn: 1094-4087.

Zhang, Z. X., Zhan, L., Xu, K., Wu, J., Xia, Y. X. & Lin, J. T. (2008). Multiwavelength fiber laser with fine adjustment, based on nonlinear polarization rotation and birefringence fiber filter. Optics Letters, Vol. 33, No. 4, pp. 324-326, Issn: 0146-9592.

Zheng, L., Vaillancourt, J., Armiento, C. & Lu, X. J. (2006). Thermo-optically tunable fiber ring laser without any mechanical moving parts. Optical Engineering, Vol. 45, No. 7, Issn: 0091-3286.

Zhou, D. Y., Prucnal, P. R. & Glesk, I. (1998). A widely tunable narrow linewidth semiconductor fiber ring laser. Ieee Photonics Technology Letters, Vol. 10, No. 6, pp. 781-783, Issn: 1041-1135.

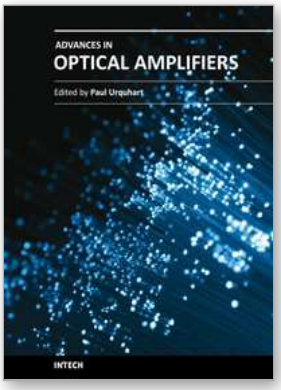

Advances in Optical Amplifiers
Edited by Prof. Paul Urquhart

ISBN 978-953-307-186-2
Hard cover, 436 pages
Publisher InTech
Published online 14, February, 2011
Published in print edition February, 2011

Optical amplifiers play a central role in all categories of fibre communications systems and networks. By compensating for the losses exerted by the transmission medium and the components through which the signals pass, they reduce the need for expensive and slow optical-electrical-optical conversion. The photonic gain media, which are normally based on glass- or semiconductor-based waveguides, can amplify many high speed wavelength division multiplexed channels simultaneously. Recent research has also concentrated on wavelength conversion, switching, demultiplexing in the time domain and other enhanced functions. Advances in Optical Amplifiers presents up to date results on amplifier performance, along with explanations of their relevance, from leading researchers in the field. Its chapters cover amplifiers based on rare earth doped fibres and waveguides, stimulated Raman scattering, nonlinear parametric processes and semiconductor media. Wavelength conversion and other enhanced signal processing functions are also considered in depth. This book is targeted at research, development and design engineers from teams in manufacturing industry, academia and telecommunications service operators.

How to reference
In order to correctly reference this scholarly work, feel free to copy and paste the following:

Feng Xiao, Kamal Alameh and Yong Tak Lee (2011). Tunable Fibre Lasers Based on Optical Amplifiers and an Opto-VLSI Processor, Advances in Optical Amplifiers, Prof. Paul Urquhart (Ed.), ISBN: 978-953-307-186-2, InTech, Available from: http://www.intechopen.com/books/advances-in-optical-amplifiers/tunable-fibre-lasers-based-on-optical-amplifiers-and-an-opto-vlsi-processor

INTECH
open science | open minds

InTech Europe
University Campus STeP Ri
Slavka Krautzeka 83/A
51000 Rijeka, Croatia
Phone: +385 (51) 770 447
Fax: +385 (51) 686 166
www.intechopen.com

InTech China
Unit 405, Office Block, Hotel Equatorial Shanghai
No.65, Yan An Road (West), Shanghai, 200040, China
中国上海市延安西路65号上海国际贵都大饭店办公楼405单元
Phone: +86-21-62489820
Fax: +86-21-62489821